

Integral-field spectroscopy of a Lyman-Break Galaxy at $z=3.2$: evidence for merging

N. P. H. Nesvadba^{1,2}, M. D. Lehnert¹, R. I. Davies³, A. Verma⁴, F. Eisenhauer³

¹ Observatoire de Paris, CNRS, Universite Denis Diderot; 5, Place Jules Janssen, 92190 Meudon, France

² Marie-Curie Fellow

³ Max-Planck-Institut für Extraterrestrische Physik, Garching bei München, Germany

⁴ University of Oxford, Subdepartment of Astrophysics, Denys Wilkinson Building, Keble Road, Oxford, UK.

Received / Accepted

ABSTRACT

We present spatially-resolved, rest-frame optical spectroscopy of a $z \sim 3$ Lyman-break galaxy (LBG), Q0347-383 C5, obtained with SINFONI on the VLT. This galaxy, among the $\sim 10\%$ brightest LBGs, is only the second $z \sim 3$ LBG observed with an integral-field spectrograph. It was first described by Pettini et al. (2001), who obtained WFPC2 F702W imaging and longslit spectroscopy in the K-band. We find that the emission line morphology is dominated by two unresolved blobs at a projected distance of ~ 5 kpc with a velocity offset of ~ 33 km s⁻¹. Velocity dispersions suggest that each blob has a mass of $\sim 10^{10} M_{\odot}$. Unlike Pettini et al. (2001), our spectra are deep enough to detect H β , and we derive star-formation rates of $\sim 20 - 40 M_{\odot} \text{ yr}^{-1}$, and use the H β /[OIII] ratio to crudely estimate an oxygen abundance $12 + [O/H] = 7.9 - 8.6$, which is in the range typically observed for LBGs. We compare the properties of Q0347-383 C5 with what is found for other LBGs, including the gravitationally lensed “arc+core” galaxy (Nesvadba et al. 2006), and discuss possible scenarios for the nature of the source, namely disk rotation, a starburst-driven wind, disk fragmentation, and merging of two LBGs. We favor the merging interpretation for bright, extended LBGs like Q0347-383 C5, in broad agreement with predicted merger rates from hierarchical models.

Key words. cosmology: observations — galaxies: evolution — galaxies: kinematics and dynamics — infrared: galaxies

1. Introduction

Our understanding of high-redshift galaxies is growing at a rapid pace. By combining ground and space-based observations, all of the electromagnetic spectrum from the X-rays to the radio is now being used to select and study galaxies in the early universe. Among the ever-growing number of high-redshift galaxy populations, Lyman Break Galaxies (LBGs) play a dominant role, from an astrophysical and from an observational point of view. Recently, Reddy et al. (2007) argued that blue, star-forming galaxies like LBGs may have had the largest contribution to the bolometric energy output of galaxies at redshifts $z \sim 2 - 3$, emphasizing their importance for our understanding of the cosmic star-formation history. Observationally, more than 1000 LBGs have spectroscopic redshifts at $z \sim 3$ alone (e.g., Steidel et al. 2003), and their ensemble properties, like their spatial clustering, luminosity function, and average rest-frame UV spectral properties are known at unprecedented precision (e.g., Adelberger et al. 2005b; Shapley et al. 2001; Papovich et al. 2001; Shapley et al. 2003). Very recently, Law et al. (2007a) presented adaptive-optics assisted integral-field spectroscopy of the $z = 3.3$ LBG DSF2237a-C2 using OSIRIS on the Keck telescope.

The picture that emerges from these observations is far from simple. Law et al. (2007a) point out that at resolutions of ~ 1 kpc reached with adaptive optics, UV-selected $z \sim 2 - 3$ galaxies have irregular kinematics, which are likely not dominated by large-scale gravitational motion, but perhaps are more related to merging

or gas-cooling. Genzel et al. (2006); Förster Schreiber et al. (2006) however argue that at least a subsample of blue, star-forming galaxies at somewhat lower redshifts, $z \sim 2$, may show the signs of large, spatially-extended, rotating disks. Distinguishing between the two scenarios is difficult, due to the low spatial resolution of the data relative to the size of the targets (see also Kronberger et al. 2007).

Here we present a study of one of the first $z \sim 3$ LBGs described in the literature, Q0347-383 C5, which was initially described by Steidel et al. (1996). With $\mathcal{R} = 23.82$ mag, Q0347-383 C5 is within the tail of the $\sim 10\%$ brightest LBGs. WFPC2 imaging shows a relatively complex morphology, extending over $\sim 1''$ down to the faint surface brightness detection limit of the image (18000s through the F702W filter) and a half light radius about a few tenths of an arc second Pettini et al. (2001). Extents this large are not rare among the bright LBG population (Conselice et al. 2003) and its half-light radius is also rather typical (Ferguson et al. 2004). Pettini et al. (2001) obtained longslit spectroscopy in the K-band for a small sample of $z \sim 3$ LBGs, including Q0347-383 C5, which was one out of two of their sources with spatially-extended spectra and a velocity gradient of ~ 70 km s⁻¹ in the [OIII] $\lambda\lambda 4959, 5007$ emission line. They placed a 3σ limit on H β of $F(H\beta) < 1.7 \times 10^{-17}$ erg s⁻¹ cm⁻².

Using the near-infrared spectrograph SINFONI on the VLT, we obtained deep, spatially-resolved spectroscopy of the [OIII] $\lambda\lambda 4959, 5007$, and H β emission line. This is only the second unlensed LBG with integral-field spectroscopy

in the literature with such observations (Law et al. 2007a, discuss the $z=3.2$ LBG DSF2238a-C2, for which they obtained rest-frame optical integral-field spectroscopy using OSIRIS on the Keck with a laser guide star.) Given the small number of LBGs with integral-field spectroscopy, and the large observational expense of such observations, even the study of a single object is already a significant step forward. Such observations overcome many uncertainties related to longslit spectroscopy, such as slit-losses, and allow us to trace the emission line morphology and kinematics across the two-dimensional surface of the target. This makes them particularly suited to disentangle the often complex emission line morphology of high-redshift galaxies.

Throughout the paper we adopt a flat $H_0 = 70 \text{ km s}^{-1} \text{ Mpc}^{-3}$ concordance cosmology with $\Omega_\Lambda = 0.7$ and $\Omega_M = 0.3$. In this cosmology, $D_L = 28 \text{ Gpc}$ and $D_A = 1.5 \text{ Gpc}$ at $z=3.23$. The size scale is $7.5 \text{ kpc arcsec}^{-1}$. The age of the universe at this redshift and cosmological model is 1.9 Gyr .

2. Observations and data reduction

We obtained deep, seeing-limited K-band spectroscopy of the $z=3.2$ LBG Q0347-383 C5, using the integral-field spectrograph SINFONI (Eisenhauer et al. 2003; Bonnet et al. 2004) on the VLT in December 2004 under excellent and stable conditions. SINFONI is a medium-resolution, image-slicing integral-field spectrograph, with $8'' \times 8''$ field of view at a $0.125'' \times 0.125''$ pixel scale and spectral resolving power $R \sim 4000$ in the K band. The total observing time was 14400s with individual exposure times of 600s. This corresponds to the on-source observing time, since we adopted a dither pattern where the galaxy was constantly within the field of view.

We used the IRAF (Tody 1993) standard tools for the reduction of longslit-spectra, modified to meet the special requirements of integral-field spectroscopy, and complemented by a dedicated set of IDL routines. Data are dark-frame subtracted and flat-fielded. The position of each slitlet is measured from a set of standard SINFONI calibration data, measuring the position of an artificial point source. Rectification along the spectral dimension and wavelength calibration are done before night sky subtraction to account for some spectral flexure between the frames. Curvature is measured and removed using an arc lamp, before shifting the spectra to an absolute (vacuum) wavelength scale with reference to the OH lines in the data. To account for variations in the night sky emission, we normalize the sky frame to the average of the object frame separately for each wavelength before sky subtraction, correcting for residuals of the background subtraction and uncertainties in the flux calibration by subsequently subtracting the (empty sky) background separately from each wavelength plane.

The three-dimensional data are then reconstructed and spatially aligned using the telescope offsets as recorded in the header within the same sequence of 6 dithered exposures (about one hour of exposure), and by cross-correlating the line images from the combined data in each sequence, to eliminate relative offsets between different sequences. Telluric correction is applied to each individual cube before the cube combination. Flux scales are obtained from standard star observations taken every hour at similar position and air mass as the source.

We also used the standard star to carefully monitor the seeing during observations, and we find an effective seeing in the combined cube of $\text{FWHM } 0.55'' \pm 0.05'' \times 0.49'' \pm 0.04''$. The spectral resolution was measured from night-sky lines and is $\text{FWHM} = 103 \text{ km s}^{-1}$ at the wavelength of $[\text{OIII}]\lambda 5007$.

2.1. Additional data sets and alignment

We also obtained WFPC2 F702W imaging of Q0347-383 C5 from the HST archive, which was originally presented by Pettini et al. (2001). We used the OTFC calibrated data sets, and followed the standard DRIZZLE procedures given in, e.g., Koekemoer (2002), to remove cosmic rays and to align and combine the individual frames.

It is difficult to accurately align the SINFONI and WFPC2 data at sub-arcsecond precision, because of the small field of view of SINFONI of only $8'' \times 8''$ and the small source size, which is about similar to the uncertainty in the absolute astrometry of both the VLT and WFPC2 ($\sim 1''$). Moreover, the morphologies in the WFPC2 continuum image and SINFONI line image are very different.

We therefore base the alignment on astrophysical arguments. Overall, the emission line regions will roughly align with the continuum, as typically observed in blue, star-forming galaxies at redshifts $z \sim 2$ (Förster Schreiber et al. 2006; Law et al. 2007a; Nesvadba et al. 2007). The only high-redshift galaxies, where the line and continuum emission do not seem to align well, are radio galaxies in which several $10^{10} M_\odot$ of ionized gas extend over radii of $\sim 20 - 30 \text{ kpc}$, which appear to be entrained and ionized by feedback from the powerful AGN (Nesvadba et al. 2007). But those can hardly be good analogs to Q0347-383 C5.

If we align the unresolved, bright knot in the southern part of the source with one of the unresolved knots in the $[\text{OIII}]\lambda 5007$ emission line image, the line and continuum emission are overall well aligned. Astrophysically, this particular choice relies on the assumption that the strong line emission and UV continuum originate from the same region, which is a reasonable assumption for both star-forming regions, and AGN. The spatial extent of the line and continuum emission are well matched, which may serve as a heuristic justification of the method, and this choice does not have a strong impact on our overall interpretation. We note that the distance between the two knots in the line image does not correspond to the distance between the faint source towards the north, which is marginally detected in the WFPC2 image, and any part of Q0347-383 C5.

3. Spatially-resolved integral-field spectroscopy of a Lyman-Break Galaxy at $z=3.2$

3.1. Continuum and emission line morphology

Q0347-383 C5 is one of the largest $z \sim 3$ LBGs, in particular it is large enough to be spatially resolved with seeing-limited observations. Fig. 1 shows the F702W morphology obtained with the HST. At $z=3.23$, the F702W bandpass corresponds to rest-frame wavelengths of $\sim 1470 - 1800 \text{ \AA}$. The brightest emission comes from a compact, marginally resolved knot, which has an intrinsic size of $0.13'' \times 0.18''$ ($0.97 \text{ kpc} \times 1.49 \text{ kpc}$ for our cosmology). We obtained this estimate from assuming that the observed full width at half maximum of the image is a quadratic sum of the intrinsic

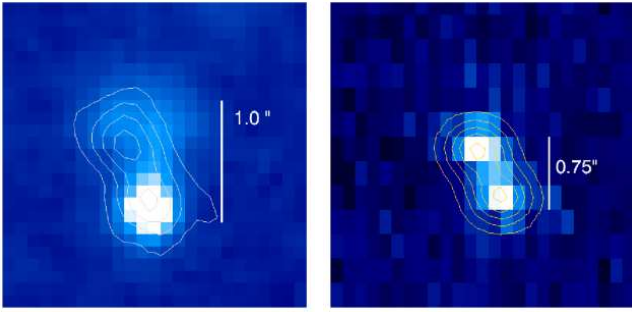


Fig. 1. *left:* [OIII] λ 5007 rest-frame UV morphology observed with WFPC2 through the F702W filter first presented by Pettini et al. (2001). The contours indicate the [OIII] λ 5007 emission line morphology extracted from our SINFONI data cube. *right:* [OIII] λ 5007 emission line morphology of Q0347-383 C5. For comparison, contours indicate the morphology of two artificial point-sources at the position of each knot in the [OIII] line image convolved with two-dimensional Gaussian distributions with widths corresponding to the spatial resolution of the data.

FWHM of the source and the point spread function, $0.1'' \times 0.1''$, which we measured from a nearby star on the same chip. The knot is separated by $\sim 0.6''$ (4.5 kpc) from a more diffuse, elongated object. About $1.6''$ (12 kpc) to the north-west from the brightest knot is another diffuse source, which is marginally detected in the WFPC2 image.

We show the [OIII] λ 5007 emission line morphology of Q0347-383 C5 in Figure 1. The image includes wavelengths ± 1 FWHM around the peak integrated emission. The emission is clearly spatially extended over an area of $\sim 0.6'' \times 1.3''$, corresponding to ~ 4.5 kpc \times 9.8 kpc. We identify two separated, unresolved line emitters at a projected distance $d_{proj} \sim 0.7''$ or 5.3 kpc. Each of the knots is spatially unresolved (see right panel of Fig. 1 which shows the line distribution compared to a point source), and we place upper limits on their size from the size of the seeing disk, finding FWHM of $< 2.7 \times 2.3$ kpc in right ascension and declination, respectively. We do not detect any line emission from the diffuse, faint continuum source to the north west.

3.2. Integrated spectrum

The integrated spectrum of Q0347-383 C5 is shown in the inset of Fig. 2. The spectrum was integrated by summing over all spatial pixels in which the [OIII] λ 5007 emission exceeds 3σ . The redshift is $z=3.2347 \pm 0.0007$. The [OIII] $\lambda\lambda$ 4959,5007 doublet is very prominent, and detected at 5σ and 12σ , respectively. Our results on the redshift, FWHM, and line flux of [OIII] agree with those of Pettini et al. (2001), but unlike Pettini et al., we also detect $H\beta$ with a flux of $F_{H\beta} = 8.8 \pm 1.8 \times 10^{-18}$ erg s^{-1} cm^{-2} . This flux is consistent with the 3σ upper limit given by Pettini et al. (2001). We find a [OIII]/ $H\beta$ flux ratio of $[OIII]_{5007}/H\beta = 7.2 \pm 1.5$. Line widths are $FWHM_{5007} = 180 \pm 9$ km s^{-1} for [OIII] λ 5007, and $FWHM_{H\beta} = 69 \pm 11$ km s^{-1} for $H\beta$, respectively. The lower $H\beta$ line width may be due to its unlucky wavelength with respect to the telluric absorption.

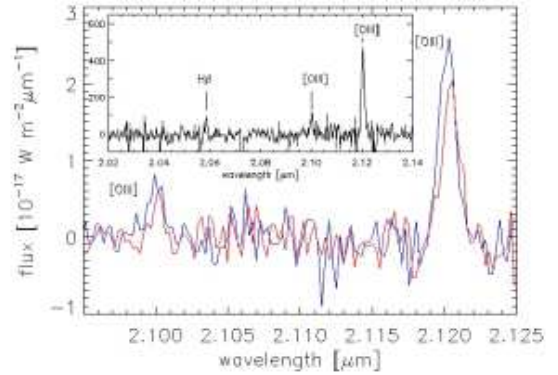


Fig. 2. Individual spectra of knot A and B are shown as red and blue curve, respectively. Both components have very similar spectral properties, and a relative velocity shift of 33 ± 10 km s^{-1} . The inset shows the integrated spectrum of Q0347-383 C5 extracted from our SINFONI data cube. $H\beta$ and the [OIII] $\lambda\lambda$ 4959,5007 doublet are clearly detected.

We use the integrated spectrum to give a rough R_{23} -like metallicity estimate for Q0347-383 C5. We did not measure the [OII] $\lambda\lambda$ 3726,3729 doublet, therefore, we use the correlation of [OII] λ 3727/[OIII] λ 5007 with [OIII] λ 5007/ $H\beta$ given by Kobulnicky et al. (1999) for low-metallicity galaxies to estimate the most likely [OII] λ 3727 flux. With the measured uncertainties and the $\log([OII]/H\beta) = 0.4$ suggested by the Kobulnicky et al. correlation, $R_{23} = 1.05$. If instead we only use the measured [OIII] and $H\beta$ values, and neglect any contribution from [OII], we find $R_{23,OIII} = 0.95$. This corresponds to a highly conservative, but probably very loose lower bound. Including the 1σ uncertainties of our flux measurements, this corresponds to $R_{23} > 0.86$, or a metallicity between 8.6 and 7.9.

This estimate may appear relatively uncertain, but we emphasize that this is the case for any metallicity estimate of high-redshift galaxies from emission lines. Even the sample of Pettini et al. (2001), which had measured [OII] λ 3727, [OIII] $\lambda\lambda$ 4959,5007, and $H\beta$ fluxes, could not be corrected for extinction, which will introduce considerable uncertainties. With these caveats in mind, Q0347-383 C5 has an oxygen abundance similar to those of the subsample of Pettini et al. (2001) with R_{23} measured. Comparing with the solar oxygen abundance estimate of Allende Prieto et al. (2001), $[O/H] = 8.69 \pm 0.05$, we find that Q0347-383 C5 has a mildly subsolar metallicity ranging $[M/H] \sim -0.1 - -0.7$ dex.

3.3. Spatially-resolved kinematics and properties of individual knots

To map the velocity and dispersion fields, we extracted the [OIII] λ 5007 emission lines from 3×3 pixel apertures ($0.375'' \times 0.375''$), which is below the seeing disk. In addition, we smoothed the spectra over 3 pixels along the spectral axis. The result is shown in Fig. 3. Typical uncertainties are $\sim 10 - 15$ km s^{-1} in both maps. Velocities between the two components are significantly different, and do not vary smoothly, but change abruptly near the mid point between the knots. Velocities in each individual knot are very uniform across the full two-dimensional surface.

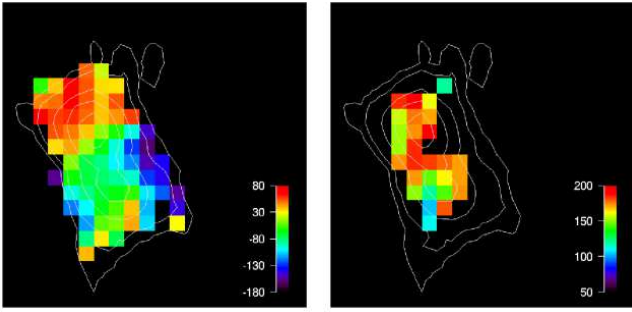


Fig. 3. The velocity and width map of Q0347-383 C5 are shown in the left and right panel, respectively. The velocity does not vary smoothly across the source, but abruptly between the two knots. Line widths are uniform across the source. Color bars indicate the velocities and FWHM line widths in km s^{-1} in the left and right panel, respectively.

The [OIII] morphology further suggests that most of the line emission comes from the two knots, with a negligible contribution from more diffuse, extended areas. This correspondence between the two-dimensional morphology and velocity map suggests that Q0347-383 C5 is composed of two individual components, each dominated by its internal kinematics. FWHM line widths are relatively uniform, and are marginally lower in the northern component. Towards north-west, lines are not resolved spectrally.

We extracted spectra from each individual knot, finding that both have very similar properties (Fig. 2). For knot *A* and *B*, we find line widths of $\text{FWHM}_A = 207 \pm 7 \text{ km s}^{-1}$ and $\text{FWHM}_B = 181 \pm 3 \text{ km s}^{-1}$, respectively, and a velocity offset between the two integrated spectra of $\Delta v = 33 \pm 10 \text{ km s}^{-1}$. We observe a similar offset in both lines of the [OIII] $\lambda\lambda 4959, 5007$ doublet. $\text{H}\beta$ is detected in both components, with fluxes of $F_A(\text{H}\beta) = 6.6 \pm 1.8 \times 10^{-21} \text{ W m}^{-2}$ and $F_B(\text{H}\beta) = 5.7 \pm 1.8 \times 10^{-21} \text{ W m}^{-2}$ in components *A* and *B*, respectively. Oxygen ratios in the two knots are similar within the (relatively large) uncertainties, suggesting subsolar metallicities in both components.

We use the measured velocity dispersions, corrected for the instrumental resolution, of each knot to give a rough estimate of the mass of each component, assuming that each knot has a King profile and setting $M = c \sigma^2 R/G$ with dynamical mass, M , velocity dispersion, σ , radius, R , and gravitational constant, G . c is a correction factor, with $c \sim 4 - 6$ for early-type galaxies on the fundamental plane, depending on the ratio between tidal radius and core radius (Bender et al. 1992). For simplicity, and since we are not able to constrain this ratio from our observations, we assume $c = 5$. The additional uncertainty does not dominate the overall error budget of our mass estimate. The FWHMs given in §3.3 correspond to velocity dispersions in the two knots of $88 \pm 3 \text{ km s}^{-1}$ and $77 \pm 3 \text{ km s}^{-1}$ (§3), respectively, and we use the upper limits on the size of each clump, $\text{HWHM} \leq 1.4 \text{ kpc}$. Thus, we find $M_A \lesssim 9 \times 10^9 M_\odot$ and $M_B \lesssim 1.2 \times 10^{10} M_\odot$ for component *A* and *B*, respectively. Note that Pettini et al. (2001) used the same method to estimate the average dynamical mass of LBGs, for an average radius of 2.5 kpc.

If alternatively, we assume that the velocity dispersion in each knot is dominated by disk rotation, then we can set $M = v^2 R/G$, with circular (and deprojected) velocity

$v = f_c \times v_{\text{obs}}$, corresponding to the observed velocity, v_{obs} , corrected by a factor $f_c = 1.7$, for an average inclination and the apparent flattening of the rotation curve due to the seeing (Rix et al. 1997). We find $M_A = 5 \times 10^9 M_\odot$ and $M_B = 7 \times 10^9 M_\odot$, respectively.

Having detected $\text{H}\beta$, we can estimate star-formation rates in each knot, following Kennicutt (1998) and adopting a Balmer decrement of $\text{H}\alpha/\text{H}\beta = 2.86$. For a Salpeter IMF and mass range of $1 - 100 M_\odot$, this corresponds to a conversion of star-formation rate, SFR, to emission line luminosity, $\mathcal{L}_{\text{H}\beta}$, of $\text{SFR} [M_\odot \text{ yr}^{-1}] = \mathcal{L}_{\text{H}\beta} [3.7 \times 10^{34} \text{ W}]$. For components *A* and *B*, respectively, we find star formation rates $\text{SFR}_A = 14 M_\odot \text{ yr}^{-1}$ and $\text{SFR}_B = 12 M_\odot \text{ yr}^{-1}$. These values were derived with the assumption that extinction in Q0347-383 C5 is negligible and therefore our estimates correspond to lower limits. Shapley et al. (2001) found for their LBG sample $\text{E(B-V)} = 0.2-0.4$, indicating that intrinsic fluxes may be factors 1.6-3 higher (for a galactic extinction law). We therefore do not expect that extinction corrected rates will greatly exceed $\text{SFR}_A \sim 19 - 35 M_\odot \text{ yr}^{-1}$ and $\text{SFR}_B \sim 22 - 42 M_\odot \text{ yr}^{-1}$ for components *A* and *B*, respectively. Using the observed G-R color of Q0347-383 C5, $\text{G-R} = 0.65 \text{ mag}$, and for a constant starburst with an age of a few 10^7 years, we expect extinctions that are even lower, $\text{E(B-V)} < 0.1$.

4. Q0347-383 C5 – Formation, outflow, or rotation?

Integral-field spectroscopy (e.g. Law et al. 2007a; Förster Schreiber et al. 2006) and longslit spectroscopy (Erb et al. 2003) revealed that galaxies at $z \sim 2 - 3$ often have complex kinematics that are not easily interpreted. While Law et al. (2007a) highlight the small observed ratios between velocity gradient and total dispersion, v/σ , of many of the most extended sources, and suggest that this may be due to processes more complex than simple self-gravitating disks, Förster Schreiber et al. (2006); Genzel et al. (2006) argue for rotation of large-scale disks in at least a subset, the best observed subset, of their sample. Evidence for rotation on sub-kpc scales, has been found by Nesvadba et al. (2006b) in a gravitationally lensed, strongly magnified arc at $z=3.24$. Alternatively, the gas kinematics may be influenced by feedback from star-formation or AGN. We will in the following discuss these possible interpretations.

4.1. The wind scenario

Many LBGs show blue asymmetries in the profiles of their rest-frame optical emission lines (Nesvadba et al. 2007). Generally, in actively star-forming galaxies, such asymmetries are interpreted as a sign of starburst-driven outflows of ionized gas (Lehnert & Heckman 1996). Similar outflows are expected in galaxies with star-formation densities $> 0.1 M_\odot \text{ yr}^{-1} \text{ kpc}^{-2}$ (Heckman 2003), and most LBGs easily surpass this limit. The star-formation intensities in Q0347-383 C5 are above this limit ($> 2 M_\odot \text{ yr}^{-1} \text{ kpc}^{-2}$, corresponding to the observed HWHM to approximate the radius, and the measured star-formation rate, $\text{SFR}_B = 12 M_\odot \text{ yr}^{-1}$, in component *B*).

However, the [OIII] $\lambda 5007$ line wings do not show well-pronounced blue wings, and the [OIII] emission line mor-

phology in Fig. 1 does not suggest that the overall line emission is dominated by a wind. The line emission is concentrated in two knots that are each spatially unresolved. In contrast, the morphologies of starburst-driven winds at low redshift (e.g., Lehnert & Heckman 1996) typically resemble edge-brightened bubbles in the line emission that have “broken out” of the confinement provided by the ambient ISM.

Moreover, starburst-driven winds have typically low surface brightness at low redshift (Lehnert & Heckman 1996) and even in massive starbursts at high redshift in spatially-resolved data sets. For the submillimeter selected $z=2.6$ galaxy SMMJ14011+0252 with a star-formation rate of a few $\times 100 M_{\odot} \text{ yr}^{-1}$, Nesvadba et al. (2007) find that starburst-driven winds do overall not dramatically alter the observed, large-scale kinematics of the galaxy, but have a measurable influence on the line profiles of the optical emission lines.

Comparison with the rest-frame UV absorption line spectrum yields similar conclusions. Pettini et al. (2001) give redshifts for $\text{Ly}\alpha$ and the interstellar absorption lines for Q0347-383 C5 of $z(\text{Ly}\alpha) = 3.244$ and $z(\text{abs}) = 3.236$, respectively. While redshifted $\text{Ly}\alpha$ and interstellar lines relative to the rest-frame optical emission lines are commonly interpreted as evidence for outflows of neutral and ionized gas, in Q0347-383 C5, both $\text{Ly}\alpha$ and rest-frame UV absorption lines have redshifts relative to the rest-frame optical emission line gas. This may indicate more complex kinematics of the neutral and ionized material, perhaps related to infalling gas, or to a variety of physical processes affecting the kinematics of different components of the gas in LBGs.

4.2. The rotating disk scenario

Empirically, rotation curves of low redshift galaxies exhibit a large range of shapes, and in spite of a large number of attempts (e.g., Persic & Salucci 1991), there is no single expression that is adequate to describe the velocity gradients of rotationally-supported galaxies with a “unified” rotation curve. This certainly adds to the uncertainty in interpreting the observed velocity gradients in high redshift galaxies as rotation, in particular when the gradient may only be apparently smooth as a consequence of low spatial resolution.

Nesvadba et al. (2006a) find strong evidence for rotation within the central kpc (and likely out to radii of a few kpc) of a strongly lensed LBG at $z=3.2$ – the “arc+core” galaxy. In particular, they find that the velocity profile in the central kpc of the “arc+core” galaxy is nearly indistinguishable from the rotation curve of the low-redshift spiral galaxy NGC4419. Contrary to the arc+core, Q0347-383 C5 has a light profile consistent with two spatially unresolved knots, with an abrupt velocity change inbetween, which is not suggestive of an isolated rotating disk on the scales of a few kpc that we spatially resolve.

4.3. The merger scenario

Based on the emission line morphology and kinematics of Q0347-383 C5, we favor the merger scenario. With a separation of ~ 5 kpc, the two knots in the emission line image may well be the sites of two giant star-forming regions, perhaps nuclear starbursts in two interacting or merging

galaxies. Alternatively, the knots may represent two sub-clumps formed in a massive, collapsing gas disk, as discussed by Immeli et al. (2004) and Bournaud et al. (2007). Depending on the initial mass and the efficiency of energy dissipation of the cold component, the gas is more or less likely to fragment due to instabilities within an underlying disk. Bournaud et al. (2007) argue that this may be a mechanism to explain the irregular, clumpy morphologies of chain and clump-cluster galaxies. These disk instability models imply disks with numerous small clumps with 10s of parsecs in size and small masses, to only several but individually large, 1-2 kpc, more massive ($\sim 10^{8-9} M_{\odot}$) clumps (Immeli et al. 2004; Bournaud et al. 2007).

Distinguishing between a galaxy merger and the merger of two massive subclumps embedded within a rotating disk is difficult, but we can give a tentative answer from our measurements of the velocity dispersion, estimates of the mass, and upper limits to the sizes of the individual components within Q0347-383 C5.

LBGs have dynamical masses of on average $\sim 10^{10} M_{\odot}$ (Pettini et al. 2001; Nesvadba et al. 2006a). Given that the properties of Q0347-383 C5 are rather typical of other LBGs and that the two components have relatively similar velocity dispersions, we suspect that our estimated upper limits to the masses are also within a factor of a few of their actual masses. Observed line widths in the integrated spectrum of the lensed “arc+core” on physical scales of ~ 200 pc are very similar ($\sigma = 97 \pm 7 \text{ km s}^{-1}$ Nesvadba et al. 2006a), while those observed in $z \sim 2$ galaxies by Law et al. (2007a); Förster Schreiber et al. (2006) are in many cases significantly larger. This suggests that the line widths we observe are representative for the overall widths in the two knots, and are not an artifact due to the blended kinematics of neighboring, self-gravitating clouds.

Given the similarities between each component of Q0347-383 C5 and other LBGs, we favor the interpretation that Q0347-383 C5 consists of two individual galaxies. Each of these clumps is likely higher in mass, about a factor of 10 than expected for clumps, and certainly each has a higher velocity dispersion, $\sim 90 \text{ km s}^{-1}$, compared to 20-30 km s^{-1} for the most massive clumps predicted in the models simulating disk instability (Immeli et al. 2004). The small projected distance of $d_{proj} \sim 5$ kpc and small velocity offset of $\sim 33 \pm 10 \text{ km s}^{-1}$, smaller than the velocity dispersion of each component, make it unlikely that they lie in a disk configuration, again suggesting that it is most likely that Q0347-383 C5 represents a pair of LBGs that will probably merge within the next few 100 Myrs.

Interestingly, the rest-frame UV absorption lines (Steidel et al. 1996) are redshifted relative to the rest-frame optical lines, whereas $\text{Ly}\alpha$ is redshifted relative to the interstellar absorption lines. This may indicate relatively complex kinematics, with some of the gas infalling into the system. Again, this could be taken as evidence in support of the merger hypothesis, albeit not unique, since an obvious way of generating gas with a range of ionization and kinematics, including infall, is through a merger.

4.4. Is Q0347-383 C5 typical for the luminous tail of the LBG population?

Is the merger interpretation in agreement with what can be expected from the global properties of $z \sim 3$

LBGs? We address this question by comparing the number of observed LBGs with properties similar to Q0347-383 C5 with predictions from hierarchical structure formation models. Recently, Maller et al. (2006) predicted the rates of major mergers as a function of redshift and galaxy mass out to redshifts $z \sim 3$, based on smoothed-particle hydrodynamical simulations. For baryonic masses greater than $\sim 2 \times 10^{10} M_{\odot}$ they predict a merger rate of $\sim 2 - 8 \times 10^{-4} \text{Gyr}^{-1} \text{Mpc}^{-3}$, which is less than or roughly similar to the co-moving space density of LBGs brighter than $R \sim 24$ mag ($\sim 7 \times 10^{-4} \text{Mpc}^{-1}$ Adelberger & Steidel 2000; Reddy et al. 2007). Shapley et al. (2001) and Papovich et al. (2001), from population synthesis models estimate typical ages of LBGs at $z \sim 3$ to be a few 100 Myrs. This is roughly half the cosmic time spanned by the LBG selection which is about 600 Myrs (for $z \sim 2.7 - 3.4$; Steidel et al. 2003). Based on these numbers, Shapley et al. (2001) estimated that the “duty cycle” for LBGs at $z \sim 3$ is about 0.5.

For the merger hypothesis to be viable, mergers must have a similar timescale during which they could provide the characteristic age and duty cycle observed in LBGs. Interestingly, merger timescales are roughly similar to the ages of LBGs derived from population synthesis models (few $\times 10^8$ yrs, e.g., Barnes & Hernquist 1996) and thus we might expect to see about 1/2 the high redshift population at this epoch undergoing mergers if all bright LBGs have a merger phase.

This similarity between timescales and duty cycle suggests that mergers may play a significant role in the ensemble properties of the LBG population, in particular within the luminous tail of LBGs, brighter than $R \sim 24$ mag, and similar to Q0347-383 C5. Adelberger et al. (2005a) find for UV selected galaxies at $z \sim 1.8 - 3.5$, predominantly at $z \leq 2.6$, that brighter (at K-band) and redder galaxies have larger correlation lengths than the fainter ones, suggesting that the more luminous and redder galaxies may reside in more massive dark-matter halos. Following the hierarchical model, this would imply that they are presumably more massive and older than their less massive analogs. Since we did not detect the K-band continuum for Q0347-383 C5, we cannot compare directly with the Adelberger et al. results, but suspect that Q0347-383 C5 is significantly fainter than the $K=20.5$ used by Adelberger et al. to discriminate between faint and bright UV selected galaxies.

The irregularity of UV morphologies led Conselice et al. (2003) to suspect that major mergers may play an important role at these redshifts, similar to what we find for Q0347-383 C5. It appears that bright UV selected galaxies have larger numbers of UV-bright components than their fainter counterparts but that other morphological and star-formation properties (like the overall star-formation rate) do not (Law et al. 2007b; Shapley et al. 2003). While the underlying processes responsible for these trends are not unambiguously known, at least these results do not directly contradict the merger hypothesis.

However, Law et al. (2007b) point out that the absence of clear correlations between UV morphology and other parameters makes it difficult to associate a complex continuum morphology in the rest-frame UV uniquely with a merger. They suggest merger-triggered star-formation should lead to enhanced bolometric luminosity as well as UV emission from young stellar populations, which they do not find. However, these studies include “classical” LBGs

like Q0347-383 C5, but also galaxies selected with other UV-based criteria. Overall, this illustrates the difficulties related to purely morphological and photometric studies and highlights the need to include integral-field kinematics for statistically robust samples of the various high-redshift galaxy populations, if we want to understand the underlying mechanisms governing galaxy evolution in the early universe.

5. Summary and conclusions

We presented an analysis of rest-frame optical integral-field spectroscopy of the $z = 3.23$ Lyman-Break Galaxy Q0347-383 C5 in the K band. This galaxy is one of the largest known LBGs, and in particular large enough for seeing-limited observations. Q0347-383 C5 was first described by Pettini et al. (2001), who obtained F702W HST continuum imaging and longslit spectroscopy in the K-band

We detect the [OIII] $\lambda\lambda 4959, 5007$ doublet with line properties that are similar to those discussed in Pettini et al. (2001), but in addition, we also identify $H\beta$ with a flux of $9 \times 10^{-18} \text{erg s}^{-1} \text{cm}^{-2}$. The [OIII]/ $H\beta$ line ratio is high, but not too high for a low-metallicity star-forming galaxy, and corresponds to an oxygen abundance within the range of metallicities of LBGs measured by Pettini et al. (2001). The observations do not suggest that the optical spectrum of Q0347-383 C5 is dominated by an AGN.

The [OIII] $\lambda 5007$ line image shows two knots at a projected distance $\sim 0.7''$ (5.4 kpc) with a small relative velocity of 33km s^{-1} . Line morphology and kinematics do not resemble those expected for an outflow or a rotating disk, and more likely originate from a merger of either two intermediate-mass galaxies with a dynamical mass of $\leq 10^{10} M_{\odot}$ each, or perhaps massive subclumps of a fragmented disk as postulated by Immeli et al. (2004); Bournaud et al. (2007). The large masses of individual knots make it more likely that we see the merging of two galaxies each tracing its individual dark matter halo or subhalo, although this is a very difficult distinction to make with present day data. The density of similarly luminous $z \sim 3$ LBGs is consistent with predictions from recent models of the cosmic evolution of the merger rate. Star-formation rates estimated from the observed $H\beta$ flux correspond to $\sim 20 - 40 M_{\odot}$ in each clump, which is not unusual for LBGs generally.

Most $z \sim 3$ LBGs are significantly more compact than Q0347-383 C5, with typical half-light radii of $r_e \sim 0.3''$. Such scales are difficult to resolve with 10-m class telescopes, even with adaptive optics assisted observations. From such observations Law et al. (2007a) find that DSF2237a-C2, their only target at $z > 3$, has a velocity gradient and velocity dispersions of the same magnitude as the shear. While superficially these characteristics could be suggestive of a rotating disk, Law et al. (2007a), from a comparison of their data to a simple exponential rotating disk model, emphasize that this source is unlikely to be a thin, rotationally-supported disk. Both galaxies are among the largest LBGs and are comparably bright, which sheds doubts as to whether the properties of the overall population of $z \sim 3$ LBGs are well described by the properties of its largest members. Nesvadba et al. (2006a) found evidence for rotation on sub-kpc scales in a strongly-lensed LBG at $z = 3.24$, but such scales are well beyond reach for generic LBGs even with adaptive optics. While adaptive

optics-assisted observations allow to probe the dynamics of high-redshift galaxies at sub-kpc resolution, they must concentrate on galaxies with particularly bright line emission, to ensure reasonable observing times as pointed out by Law et al. (2007a).

This will inevitably lead to biases between observed LBG samples and the parent population of LBGs, and is a reason why studies of gravitationally lensed are not superseded, but are rather complemented, by high angular resolution observations of LBGs with adaptive optics, in spite of uncertainties related to the gravitational magnification. More positively, observing galaxies with bright line emission will plausibly provide information about particularly rapid phases of star-formation and galaxy growth, whatever mechanism is responsible for initiating such phases. Prudence and caution however are certainly justified when generalizing the results of high redshift galaxies given the current limitation in astronomical instrumentation and the small sample sizes with detailed 3-dimensional spectroscopy observations.

Acknowledgements. We would like to thank an anonymous referee for helpful advice and suggestions that substantially improved this paper and the staff at Paranal for their help and support in obtaining these observations. NPHN wishes to acknowledge financial support from the European Commission through a Marie Curie Postdoctoral Fellowship and MDL wishes to thank the Centre Nationale de la Recherche Scientifique for its continuing support of his research.

References

- Adelberger, K. L., Erb, D. K., Steidel, C. C., et al. 2005a, *ApJ*, 620, L75
- Adelberger, K. L. & Steidel, C. C. 2000, *ApJ*, 544, 218
- Adelberger, K. L., Steidel, C. C., Pettini, M., et al. 2005b, *ApJ*, 619, 697
- Allende Prieto, C., Lambert, D. L., & Asplund, M. 2001, *ApJ*, 556, L63
- Barnes, J. E. & Hernquist, L. 1996, *ApJ*, 471, 115
- Bender, R., Burstein, D., & Faber, S. M. 1992, *ApJ*, 399, 462
- Bonnet, H., Abuter, R., Baker, A., et al. 2004, *The Messenger*, 117, 17
- Bournaud, F., Elmegreen, B. G., & Elmegreen, D. M. 2007, *ArXiv e-prints*, 708
- Conselice, C. J., Bershady, M. A., Dickinson, M., & Papovich, C. 2003, *AJ*, 126, 1183
- Eisenhauer, F., Abuter, R., Bickert, K., et al. 2003, in Presented at the Society of Photo-Optical Instrumentation Engineers (SPIE) Conference, Vol. 4841, Instrument Design and Performance for Optical/Infrared Ground-based Telescopes. Edited by Iye, Masanori; Moorwood, Alan F. M. Proceedings of the SPIE, Volume 4841, pp. 1548-1561 (2003)., ed. M. Iye & A. F. M. Moorwood, 1548-1561
- Erb, D. K., Shapley, A. E., Steidel, C. C., et al. 2003, *ApJ*, 591, 101
- Ferguson, H. C., Dickinson, M., Giavalisco, M., et al. 2004, *ApJ*, 600, L107
- Förster Schreiber, N. M., Genzel, R., Lehnert, M. D., et al. 2006, *ApJ*, 645, 1062
- Genzel, R., Tacconi, L. J., Eisenhauer, F., et al. 2006, *Nature*, 442, 786
- Heckman, T. M. 2003, in *Revista Mexicana de Astronomia y Astrofisica Conference Series*, Vol. 17, *Revista Mexicana de Astronomia y Astrofisica Conference Series*, ed. V. Avila-Reese, C. Firmani, C. S. Frenk, & C. Allen, 47-55
- Immeli, A., Samland, M., Westera, P., & Gerhard, O. 2004, *ApJ*, 611, 20
- Kennicutt, Jr., R. C. 1998, *ARA&A*, 36, 189
- Kobulnicky, H. A., Kennicutt, Jr., R. C., & Pizagno, J. L. 1999, *ApJ*, 514, 544
- Koekemoer, A. M. e. 2002, *HST dither handbook (STScI: Baltimore)*
- Kronberger, T., Kapferer, W., Schindler, S., & Ziegler, B. L. 2007, *ArXiv e-prints*, 707
- Law, D. R., Steidel, C. C., Erb, D. K., et al. 2007a, *ArXiv e-prints*, 0707.3634
- Law, D. R., Steidel, C. C., Erb, D. K., et al. 2007b, *ApJ*, 656, 1
- Lehnert, M. D. & Heckman, T. M. 1996, *ApJ*, 472, 546
- Maller, A. H., Katz, N., Kereš, D., Davé, R., & Weinberg, D. H. 2006, *ApJ*, 647, 763
- Nesvadba, N. P. H., Lehnert, M. D., Eisenhauer, F., et al. 2006a, *ApJ*, 650, 661
- Nesvadba, N. P. H., Lehnert, M. D., Eisenhauer, F., et al. 2006b, *ApJ*, 650, 693
- Nesvadba, N. P. H., Lehnert, M. D., Genzel, R., et al. 2007, *ApJ*, 657, 725
- Papovich, C., Dickinson, M., & Ferguson, H. C. 2001, *ApJ*, 559, 620
- Persic, M. & Salucci, P. 1991, *ApJ*, 368, 60
- Pettini, M., Shapley, A. E., Steidel, C. C., et al. 2001, *ApJ*, 554, 981
- Reddy, N. A., Steidel, C. C., Pettini, M., et al. 2007, *ArXiv e-prints*, 0706.4091
- Rix, H.-W., Guhathakurta, P., Colless, M., & Ing, K. 1997, *MNRAS*, 285, 779
- Shapley, A. E., Steidel, C. C., Adelberger, K. L., et al. 2001, *ApJ*, 562, 95
- Shapley, A. E., Steidel, C. C., Pettini, M., & Adelberger, K. L. 2003, *ApJ*, 588, 65
- Steidel, C. C., Adelberger, K. L., Shapley, A. E., et al. 2003, *ApJ*, 592, 728
- Steidel, C. C., Giavalisco, M., Pettini, M., Dickinson, M., & Adelberger, K. L. 1996, *ApJ*, 462, L17+
- Tody, D. 1993, in *Astronomical Society of the Pacific Conference Series*, Vol. 52, *Astronomical Data Analysis Software and Systems II*, ed. R. J. Hanisch, R. J. V. Brissenden, & J. Barnes, 173-+